Journal of Alloys and Compounds 509 (2011) 5437–5440

Contents lists available at ScienceDirect

Journal of Alloys and Compounds

journal homepage: www.elsevier.com/locate/jallcom

Novel blue-violet photoluminescence from sputtered ZnO thin films

Zhiwen Liang [a], Xiang Yu [b], Bingfu Lei [a], Pengyi Liu [a], Wenjie Mai [a,c,*]

[a] Department of Physics and Siyuan Laboratory, Jinan University, 601 Huangpudadao, Guangzhou, Guangdong 510632, China
[b] Analytical and Testing Center, Jinan University, Guangzhou, Guangdong 510632, China
[c] Key Laboratory of Optoelectronic Information and Sensing Technologies, Jinan University, Guangzhou, Guangdong 510632, China

ARTICLE INFO

Article history:
Received 16 November 2010
Received in revised form 14 February 2011
Accepted 16 February 2011
Available online 23 February 2011

Keywords:
ZnO
Photoluminescence
Blue-violet
Thin films
Defects

ABSTRACT

Although wurtzite ZnO has a simple crystal structure, the mechanism of its photoluminescence is still controversial and this topic has attracted numerous research efforts. The polycrystalline ZnO thin films studied here were deposited on Si (1 0 0) substrate by sputtering in pure Ar atmosphere, and then thermally annealed in air at various temperatures ranging from 300 °C to 1050 °C. The photoluminescence spectra of the as-synthesized ZnO thin films exhibited some interesting results: two novel and remarkable blue-violet emission peaks around 415 nm and 440 nm were discovered, while the usual strong green emission peak at 450–550 nm was absent. These two blue-violet peaks might originate from zinc interstitial and zinc vacancy point defects, which were introduced during sputtering in a non-oxygen atmosphere. Strong blue-violet emissions of ZnO are highly desirable and they have great potential in light emitting and biological fluorescence labeling applications.

© 2011 Elsevier B.V. All rights reserved.

1. Introduction

As a direct semiconductor, ZnO has a wide band gap of 3.3–3.4 eV and a high exciton binding energy of 60 meV at room temperature, which is better than many other semiconductors, such as GaN (21 meV) and ZnSe (20 meV). Owing to these outstanding properties, ZnO has been recognized as a promising candidate for UV light-emitting diodes [1] and detectors [2], and it has aroused great research interests around the world. ZnO thin films can be fabricated by many methods, such as sol–gel process [2], chemical vapor deposition (CVD) [3], pulsed laser deposition (PLD) [4], magnetron sputtering [5]. In photoluminescence (PL), besides the strong UV emission from the near band edge, the visible emission properties of ZnO thin films are strongly dependent on their defects. ZnO thin films produced by different methods or at different conditions could introduce different kinds of defects, such as oxygen vacancies (V_O) [6,7], zinc interstitials (Zn_i) [8], zinc vacancies (V_{Zn}) [9,10], anti-sites (O_{Zn} and Zn_O) [11], and metal impurities [12]. A broad emission peak around 450–550 nm is the most frequently observed PL peak for ZnO thin films and this emission is usually attributed to deep level defects V_O or Zn_i. In addition, experiments have confirmed that these visible emissions can be tailored by varying the annealing temperature [13], doping concentration [14], or excitation wavelength [15].

In this research, the annealing-temperature-dependent morphological, structural and optical properties of as-prepared ZnO thin films have been investigated. The grain size and roughness of ZnO thin films increased when thermal temperature rose. Two novel and remarkable blue-violet emission peaks around 415 nm and 440 nm are observed in PL spectra from ZnO thin films, while the usual broad emission around 450–550 nm is absent. The blue-violet emissions of ZnO are highly desirable and they have great potential in light emitting and biological fluorescence labeling applications. However, only a few papers reported the blue emissions, and the proposed emission mechanisms are still controversial [16,17]. The blue-violet emissions from the samples reported in this article are stronger than its UV near band-edge emission (NBE). Changing the excitation wavelength has notable impact on NBE as well as these two new peaks. The agreement between experimentally obtained defect levels by PL and those predicted from previous work suggest that these two strong blue-violet emissions should originate from the zinc interstitial and zinc vacancy point defects, which are introduced during sputtering in Ar atmosphere.

2. Experimental

2.1. Materials

The polycrytalline ZnO thin films were prepared on Si (1 0 0) substrates by magnetron sputtering method. The ZnO target was purchased from Hefei Crystal Materials Technology Co., Ltd, a branch of MTI Corp. and the purity is 99.99%. The intrinsic Si (1 0 0) wafers were purchased from Tianjin Institute of Semiconductor Research, cleaned by a standard procedure, and transferred into the sputter chamber. The sputtering gas was Ar and the sputtering pressure was maintained at 1 Pa

* Corresponding author at: Department of Physics and Siyuan Laboratory, Jinan University, Guangzhou, 601 Huangpudadao, Guangdong 510632, China.
Tel.: +86 20 85224386x319; fax: +86 20 85220233.
E-mail address: wenjiemai@gmail.com (W. Mai).

0925-8388/$ – see front matter © 2011 Elsevier B.V. All rights reserved.
doi:10.1016/j.jallcom.2011.02.084

during deposition. The RF power was controlled at 80 W for 20 min and the thickness of the thin film is 500 nm. Subsequently, the as-prepared ZnO thin films were thermally annealed in air and at a series of different temperatures from 300 °C to 1050 °C for 2 h.

2.2. Characterization

The morphology and crystal structure of ZnO thin films were analyzed by atomic force microscopy (AFM), X-ray diffractometer (XRD), scanning electron microscopy (SEM) and energy dispersive spectroscopy (EDS). The room temperature PL experiment was carried out on Shimadzu RF-5301pc photoluminescence spectrometer and was used to evaluate NBE and defect emissions from the ZnO thin films.

3. Results and discussion

Fig. 1(a)–(c) shows the SEM image, the corresponding EDS spectrum and XRD spectrum of the ZnO thin film prepared by sputtering, respectively. From the SEM image, the grain size of the polycrystalline ZnO thin film is roughly estimated as 50–100 nm, and the film has a relative flat surface. The EDS spectrum confirms the existence of Zn, O and Si elements. ZnO grains on the surface of thin films tend to orient with *c* plane as the outer surface so as to minimize the surface energy; therefore polycrystalline wurtzite ZnO thin film exhibits only diffraction peaks from *c* plane (0 0 2) peak, in our XRD spectrum. XRD spectrum also shows Si (4 0 0) peak coming from the single crystal Si (1 0 0) substrate.

Fig. 2(a) presents the AFM image of the ZnO film deposited by sputtering and Fig. 2(b)–(d) demonstrate the surface evolution when ZnO thin films were treated with 2-h thermal annealing at 600, 900 and 1050 °C, respectively. The surface morphology undertakes steady and remarkable changes as the annealing temperature increases. For example, the average diameter of ZnO grains expands linearly from 79 nm to 305 nm as the sputtered sample is annealed up to 1050 °C, as shown in Fig. 1(e). Although the average grain size in Fig. 1(d) turns larger, the figure also clearly displays the coexistence of large and small grains, implying significant variance of grain sizes, and this phenomenon is consistent with the thermal coarsening process.

Room temperature and low temperature PL spectra of ZnO have been extensively studied because of its importance as well as complexity [6–18]. A typical PL spectrum of ZnO (black curve) is exhibited in Fig. 3(a), which is obtained from commercially available ZnO powders. The excitation wavelength is fixed at 300 nm here and later in this paper, unless declared otherwise. Both the sharp UV emission peak at 382 nm from the NBE and the broad peak round 450–550 nm from defect emission are observed. The

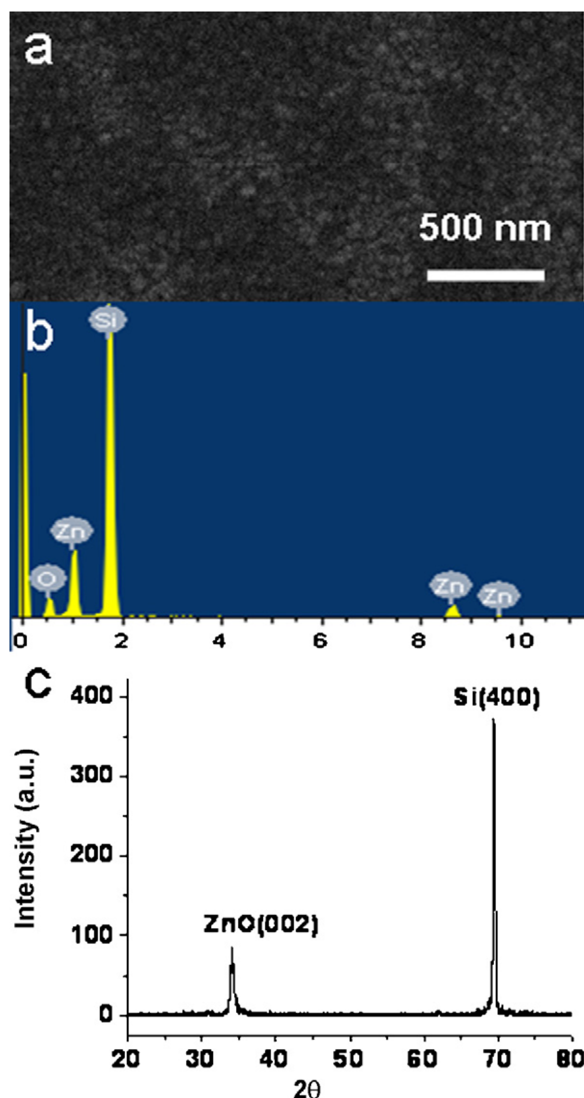

Fig. 1. (a) The SEM image of the newly sputtered ZnO thin film. (b) The EDS spectrum of the corresponding ZnO thin film, indicating existence of only Zn, O, and Si elements. (c) The XRD spectrum of the sputtered ZnO thin film, showing only ZnO wurtzite (0 0 2) and Si (4 0 0) diffraction peaks.

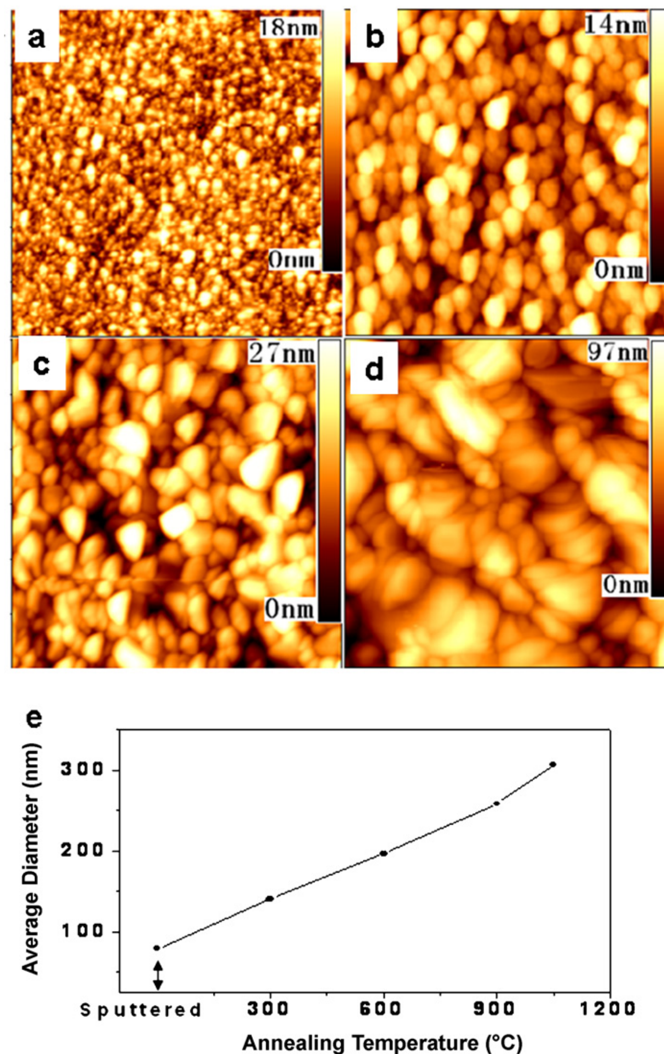

Fig. 2. (a)–(d) The AFM images of 3 μm × 3 μm area of the ZnO thin film samples, which are newly sputtered, annealed at 600, 900, and 1050 °C for 2 h, respectively. (e) The evolution of the average diameter of ZnO grains for the previous samples.

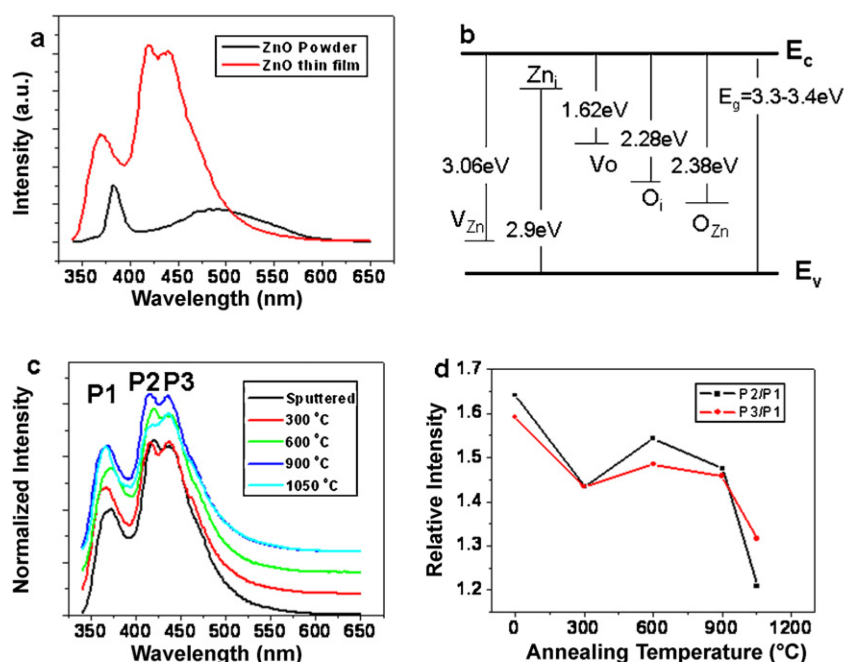

Fig. 3. (a) The PL spectra of ZnO powders (in black) and the newly sputtered ZnO thin film (in red). (b) The re-plot of the calculated defect levels in ZnO film [11]. (c) The normalized PL spectra of ZnO thin film samples (offset by a fix interval for better observation), which are sputtered, annealed at 600, 900, and 1050 °C for 2 h, respectively. (d) The relative intensity of two blue-violet emission with respect to the UV emission. (For interpretation of the references to color in this figure legend, the reader is referred to the web version of the article.)

red curve in Fig. 3(a) shows the PL spectrum of ZnO thin film sputtered from the ZnO target. The main differences between ZnO thin films and powders are described as follows: (1) for the thin film, the common green peak from defect emission is absent; (2) two novel and remarkable peaks occur in blue-violet region ∼415 nm and ∼440 nm; (3) the UV peak shifts to 370 nm. The absence of the green peak suggests the concentrations of the defects responsible for the deep level emissions are negligible. Sputtering in Ar atmosphere is believed to be a key factor in eliminating the green emission. Only a few papers reported the peaks in blue-violet region, but their PL intensity is weak for applications [16,17]. Recently, a study on PL of ZnO nanoparticles reported blue emissions at 415, 440, 455 and 488 nm (only the former two peaks are observed in our PL) in the blue wave band, and it proposed a possible mechanism related with interstitial-zinc-related defect levels as initial states for blue emission [19]. Here in this paper, another possible mechanism is discussed based on previous calculation results: a full-potential linear muffin-tin orbital method suggested that Zn_i defect level is 2.9 eV above valance band E_v and V_{Zn} defect level is 3.06 eV below conduction band E_c [11], which is also schematically plotted in Fig. 3(b). Interestingly, the blue-violet emission energy in our sample corresponds to 2.82 eV (440 nm) and 2.99 eV (415 nm), very close to 2.9 eV (Zn_i) and 3.06 eV (V_{Zn}), respectively. According to one possible defect reaction:

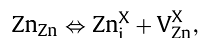

$$Zn_{Zn} \Leftrightarrow Zn_i^X + V_{Zn}^X,$$

these two kinds of defects could occur simultaneously during the sputtering process and have similar concentrations. Two novel emission peaks at 440 nm and 415 nm that have very similar intensity could be contributed by Zn_i and V_{Zn}, respectively. Concerning the UV peak shifting, different fabrication and treatment processes can cause differences in crystallinity and defect concentrations in ZnO, thus resulting in slight modification in band gap energy, which in turn shifts UV peak location.

Fig. 3(c) presents normalized PL spectra of a series of ZnO thin films that were sputtered and later thermally annealed in air at 300, 600, 900, and 1050 °C for two hours. Annealing usually can improve the crystallinity and remove partial defects. One way to evaluate the concentration of structural defects in ZnO is to compare the relative PL intensity of defect emission to the UV NBE. The impact of the annealing on the PL spectra from our samples is shown in Fig. 3(d). It is believed that annealing offers enough energy for the recombination of Zn interstitials and Zn vacancies that were induced during sputtering, and therefore relieves the blue-violet emission. Interestingly, the two peaks in blue-violet region are still larger than that of NBE, implying great potential applications in light emitting and biological fluorescence labeling. The growth of grains during annealing does not induce a systematic shift of NBE for two reasons. Firstly, when the average diameter is bigger than 10 nm, the change of band gap caused by grain size difference is neglectable. According to a formula deduced in previous literature [20,21]:

$$E_{(\mathrm{gap,nanocrystal})} = E_{(\mathrm{gap,bulk})} + \frac{\pi^2\hbar^2}{2R^2}\left(\frac{1}{m_e^*} + \frac{1}{m_h^*}\right) - 0.248E_{Ry}^*$$

where $E_{(\mathrm{gap,nanocrystal})}$ is the nanocrytsal band gap energy, $E_{(\mathrm{gap,bulk})}$ is the bulk band gap energy, E_{Ry}^* is the exciton binding energy, $\hbar$ is the reduced Planck constant, R is the radius of the grains, m_e^* is the effective electron mass, and m_h^* is the effective hole mass. The effect of average grain size is reflected in the second term on the right side. If $m_e^* = 0.24m_0$ and $m_h^* = 2.31m_0$ are adopted [21], the shift of energy is 1.04 meV when the average grain diameter increases from 79 nm to 305 nm, corresponding to 0.1 nm shift in wavelength. Secondly, two strong blue-violet emission peaks and the NBE peak overlap extensively, thus the accurate NBE peak position is hard to be determined.

In order to understand the features of the excited states related to these blue emissions, the PL spectra were carefully obtained under different excitation energies, as shown in Fig. 4. As the excitation wavelength increases from 270 nm to 330 nm with energy closer to the band gap energy of ZnO, the UV emission intensity is steadily decreasing and its location displays notable movement. In contrast, the location and intensity of the two novel blue emission peaks related to the defects remain relatively stable throughout

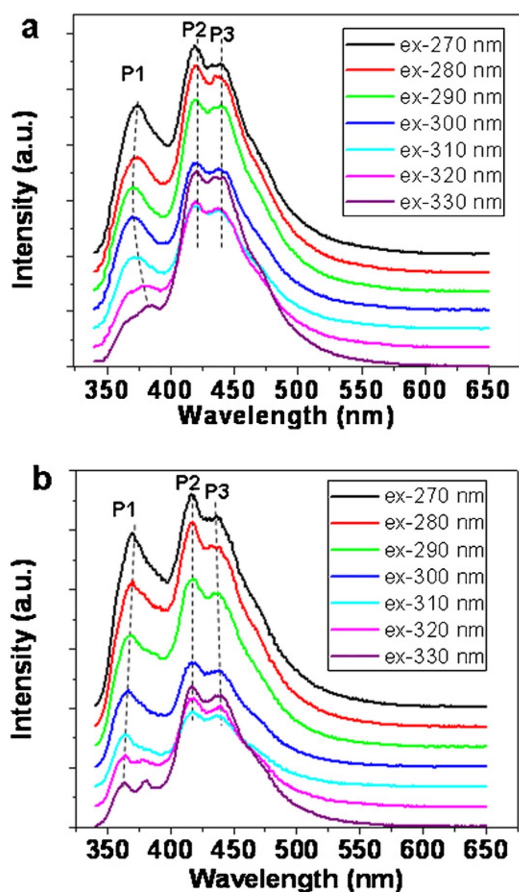

Fig. 4. Excitation-dependent PL spectra of ZnO thin film samples (offset by a fix interval for better observation), which are (a) sputtered and (b) annealed at 1050 °C for 2 h.

this series of experiments. In Fig. 4(a) for the spectra obtained from sputtered ZnO thin film, the UV emission peak slightly blue shifted from 372 nm to 370 nm, when the excitation wavelength increases from 270 nm to 310 nm. As the excitation wavelength continues increasing up to 330 nm, the UV peak reverses its shifting direction and reaches 382 nm. Similarly, when the excitation wavelength increases, UV emission diminishing effect is also observed on the sample that was annealed at 1050 °C. However, in contrast to the sample without annealing, two major differences of this annealed sample are observed: the location of original UV peak keeps blue shifting to 365 nm during increasing excitation wavelength; a new UV peak appears at 382 nm when excitation wavelength is 320 and 330 nm. One possible explanation for the observed PL characteristics is that the peak at 365 nm originates from free excitons while the peak at 382 nm from bounded excitons. When the excitation energy reduces toward the band gap energy, the NBE yield also weakens, providing better opportunity for observing separation of two weaker UV peaks. For the sample annealed at 1050 °C, the defect concentrations of zinc interstitials and zinc vacancies are reduced by thermally assisted recombination. Since there are less defects to attract and bound the excitions, the free exciton concentration in annealed sample can be enhanced and the corresponding emission can be easier for detection.

4. Conclusions

In conclusion, we have studied the morphological, structural and optical properties of a series of polycrystalline ZnO films that were annealed at various temperatures for 2 h. The grains of polycrystalline ZnO thin films experienced a coarsening process when thermal temperature rose. In PL spectra of ZnO thin film, two novel and strong blue-violet emission peaks around 415 nm and 440 nm were discovered while the usual green emission at 450–550 nm was absent. The blue-violet emissions from the samples reported in this article were stronger than their UV near band-edge emission. The origins of these two peaks might relate to the zinc interstitial and zinc vacancy point defects that were introduced during sputtering in Ar atmosphere.

Acknowledgements

This work was supported by the Natural Science Foundation of Guangdong Province, China (grant no. 10451063201005253), the Specialized Research Fund for the Doctoral Program of Higher Education of China (grant no. 20104401120005), Fundamental Research Funds for the Central Universities (grant no. 21610414), Jinan University Start-up Funds (grant no. 50624019). The authors would like to thank Prof. Chengxin Wang for helpful discussion and Dr. Hao Cui for assistance in sample characterization.

References

[1] S. Xu, C. Xu, Y. Liu, Y.F. Hu, R.S. Yang, Q. Yang, J.H. Ryou, H.J. Kim, Z. Lochner, S. Choi, R. Dupuis, Z.L. Wang, Adv. Mater. 22 (2010) 4749.
[2] K.J. Chen, F.Y. Hung, S.J. Chang, S.J. Young, J. Alloys Compd. 449 (2009) 674.
[3] W.J. Mai, P.X. Gao, C.S. Lao, Z.L. Wang, A.K. Sood, D.L. Polla, M.B. Soprano, Chem. Phys. Lett. 460 (2008) 253.
[4] A. Kaushal, D. Kaur, J. Alloys Compd. 509 (2011) 200.
[5] D.K. Kim, H.B. Kim, J. Alloys Compd. 509 (2011) 421.
[6] K. Vanheusden, C.H. Seager, W.L. Warren, D.R. Tallant, J.A. Voigt, Appl. Phys. Lett. 68 (1996) 403.
[7] T.M. Børseth, B.G. Svensson, A.Y. Kuznetsov, P. Klason, Q.X. Zhao, M. Willander, Appl. Phys. Lett. 89 (2006) 262112.
[8] M. Liu, A.H. Kitai, P. Mascher, J. Lumin. 54 (1992) 35.
[9] A.B. Djurišić, Y.H. Leung, K.H. Tam, Y.F. Hsu, L. Ding, W.K. Ge, Y.C. Zhong, K.S. Wong, W.K. Chan, H.L. Tam, K.W. Cheah, W.M. Kwok, D.L. Phillips, Nanotechnology 18 (2007) 095702.
[10] F. Tuomisto, V. Ranki, K. Saarinen, D.C. Look, Phys. Rev. Lett. 91 (2003) 205502.
[11] B.X. Lin, Z.X. Fu, Y.B. Jia, Appl. Phys. Lett. 79 (2001) 943.
[12] N.Y. Garces, L. Wang, L. Bai, N.C. Giles, L.E. Halliburton, G. Cantwell, Appl. Phys. Lett. 81 (2002) 622.
[13] S.W. Xue, X.T. Zu, W.L. Zhou, H.X. Deng, X. Xiang, L. Zhang, H. Deng, J. Alloys Compd. 448 (2008) 21.
[14] Y.X. Liu, H.L. Zhang, X.Y. An, C.T. Gao, Z.X. Zhang, J.Y. Zhou, M. Zhou, E.Q. Xie, J. Alloys Compd. 506 (2010) 772.
[15] J.H. Hong, Y.F. Wang, G. He, J.X. Wang, J. Alloys Compd. 506 (2010) 1.
[16] H.B. Zeng, W.P. Cai, J.L. Hu, G.T. Duan, P.S. Liu, Y. Li, Appl. Phys. Lett. 88 (2006) 171910.
[17] J.J. Wu, S.C. Liu, Adv. Mater. 14 (2002) 215.
[18] D.C. Reynolds, D.C. Look, B. Jogai, C.W. Litton, T.C. Collins, W. Harsch, G. Cantwell, Phys. Rev. B 57 (1998) 12151.
[19] H.B. Zeng, G.T. Duan, Y. Li, S.K. Yang, X.X. Xu, W.P. Cai, Adv. Funct. Mater. 20 (2010) 561.
[20] K. Kayanuma, Phys. Rev. B 38 (1988) 9797.
[21] S.T. Tan, B.J. Chen, X.W. Sun, W.J. Fan, J. Appl. Phys. 98 (2005) 013505.